Non-Oscillation Physics at a Neutrino Factory – VERSION 12

March 22, 2000

Introduction

version from Eric Hawker Mar 14, 2000
small mods by Mayda Velasco Mar 15, 2000
rewrite of DIS sections, Heidi Schellman, Mar 16, 2000
rewrite the introduction, structure fuctions, ew and charm, Mar 21, 2000

Due to the theoretically clean nature of weak interactions, conventional neutrino scattering experiments have always provided very precise experimental measurements of fundamental parameters. These include measurements of the Weinberg angle and the strong coupling constant α_s which are competitive with any other methods. Perhaps because of this success, we forget how crude existing neutrino experiments are. The high statistics experiments such as CDHS and CCFR/NuTeV, in order to obtain statistical samples of more that 10^5 events, rely on coarsely segmented massive iron/scintillator calorimeters weighing close to 1000 tons. Measurements on proton targets and detailed studies of the final state have been confined to very low statistics bubble chamber and electronic detectors. As a result we have virtually no precise measurements of neutrino-proton scattering and no measurements on polarized targets.

The advent of a high flux neutrino factory, with neutrino fluxes of 10^{20}/year instead of the 10^{15-16} at existing facilities would open a new era in conventional neutrino physics in which we will be able to use low mass targets and high resolution detection technologies and still achieve better statistical

power than present-day experiments. For example a 50 GeV muon storage ring would produce around 400M muon neutrino charged current interactions per year in a cubic meter of water, 200 times the statistics of the CCFR/NuTeV experiments. Better understanding of neutrino fluxes from the decay of monochromatic muons will also reduce many of the dominant systematic errors.

In this study we have concentrated on new measurements only possible with higher fluxes rather than repeating older measurements with 1000 times the statistics. As a result, the statistical errors shown are often not negligible, but without the high flux at a neutrino factor the measurements themselves would be impossible.

Outline

Due to the breadth of the field we were unable to give a complete survey and have instead highlighted a few of the areas where the high flux beam at a neutrino factory allows new measurements.

- A description of a low mass target/detector and typical rates in such a detector.
- Conventional deep inelastic scattering measurements and a proposed detector design.
- Measurements of neutrino cross sections on nuclear targets, a topic of great interest to the nuclear physics community and also needed to understand normalization at a far neutrino oscillation detector.
- Spin structure functions, which have never been measured in neutrino beams.
- The potential of the neutrino factory as a clean source of single tagged charm mesons and baryons.
- Electroweak measurements in both the hadronic and purely leptonic sectors.
- Use of the very clean initial state to search for exotic interactions
- Searches for anomalous neutrino interactions with electromagnetic fields.

Possible detector configurations and statistics

For studies of charged current deep-inelastic scattering on proton targets, the optimal detector system is probably a target followed by precision magnetic tracking sytems, an electromagnetic calorimeter and a muon detection system. Such detectors have been used in muon scattering experiments at CERN and FNAL and in the new generation neutrino scattering experiments CHORUS and NOMAD. A low mass target followed by tracking and electromagnetic calorimetry makes the electron anti-neutrinos in the beam a source of additional statistics rather than a backround, except in the case of neutral current studies.

The numerical estimates in this study use, unless otherwise noted, 10^20 50 GeV muon decays in a 600 m straight section.

The target itself should be thin enough that particles produced within it have a small probability of interacting before they reach the tracking systems. In this study we considered liquid hydrogen and deuterium targets - both polarized and unpolarized - and heavier solid nuclear targets. The hydrogen and deuterium targets are 1m long while the polarized target is 50 cm long. All targets are 20 cm in radius, to fit the central beam spot at 50 GeV. Nuclear targets are scaled so that the interaction length in the material is constant at 14%. The charge current muon neutrino interaction rates are summarized in table 1.

These are the total event rates for muon-neutrino scattering. The anti-neutrino rates are half as large. Kinematic cuts reduce the statistics by less than a factor of two. We have only considered muon-neutrino charge current scattering for structure function measurements, although for such thin targets, electron neutrino scatters should also be reconstructable with high precision.

Kinematics

The kinematic variables for neutrino deep inelastic scattering are illustrated in figure **??**:

$$\mathbf{q} = \mathbf{k}_\nu - \mathbf{k}_\ell, \qquad Q^2 = -\mathbf{q}^2 = 2E_\ell E_\nu - m_\ell^2 - 2E_\nu p_\ell \cos\theta_{lab}, \quad (1)$$

$$\nu = (\mathbf{p}_{\rm q}\mathbf{q})/ME_\ell - E'_\ell, \quad (2)$$

$$x = Q^2/2M\nu, \quad (3)$$

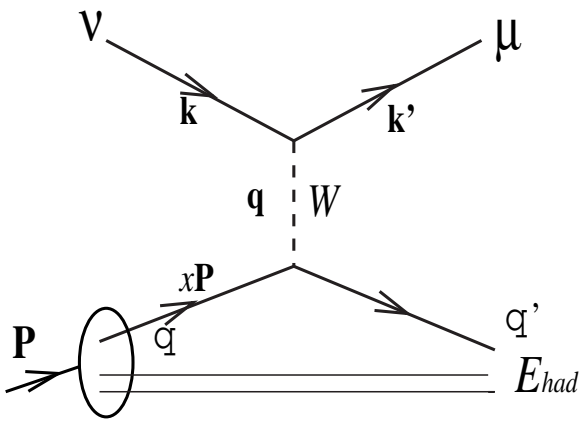

Figure 1: Kinematics of neutrino scattering in the parton model. The energy-momentum tranfer from the leptons to the proton is $\mathbf{p}_q$ and the fraction of the proton momentum carried by the struck quark is approximately x.

$$y = M\nu/(\mathbf{k}_\nu \mathbf{p}_\mathrm{q}) = (1 + cos\theta_{CM})/2 \approx \nu/E_\ell, \quad (4)$$

$$W^2 = 2M\nu + M^2 - Q^2, \quad (5)$$

where the $\mathbf{k}$ are the neutrino and final state four vectors, $\mathbf{p}_p$ is the proton four-vector, M is the target nucleon mass, E_ν is the incoming neutrino energy E_ℓ, p_ℓ are the outgoing lepton energy and momentum θ_{lab} is the lepton angle with respect to the incoming beam. $\mathbf{q}$ is the four-momentum transfer to the target, ν is the energy transfer, x is the Bjorken x variable, y is the scaled energy transfer and W^2 is the invariant mass of the final state hadronic system squared.

Figure 2 show the kinematic region for a neutrino factory as compared to other deep-inelastic scattering experiments.

0.0.1 Unpolarized Neutrino Scattering

For $Q << E$ and $s << M_W$ the the unpolarized neutrino(anti-neutrino) scattering cross section is:

$$\frac{d\sigma^{\nu(\overline{\nu})}}{dxdy} = \frac{G_F^2 M E_\nu}{2\pi}\Big[[F_2(x,Q^2) \pm xF_3] + [F_2(x,Q^2) \mp xF_3(x,Q^2)](1-y)^2 \quad (6)$$

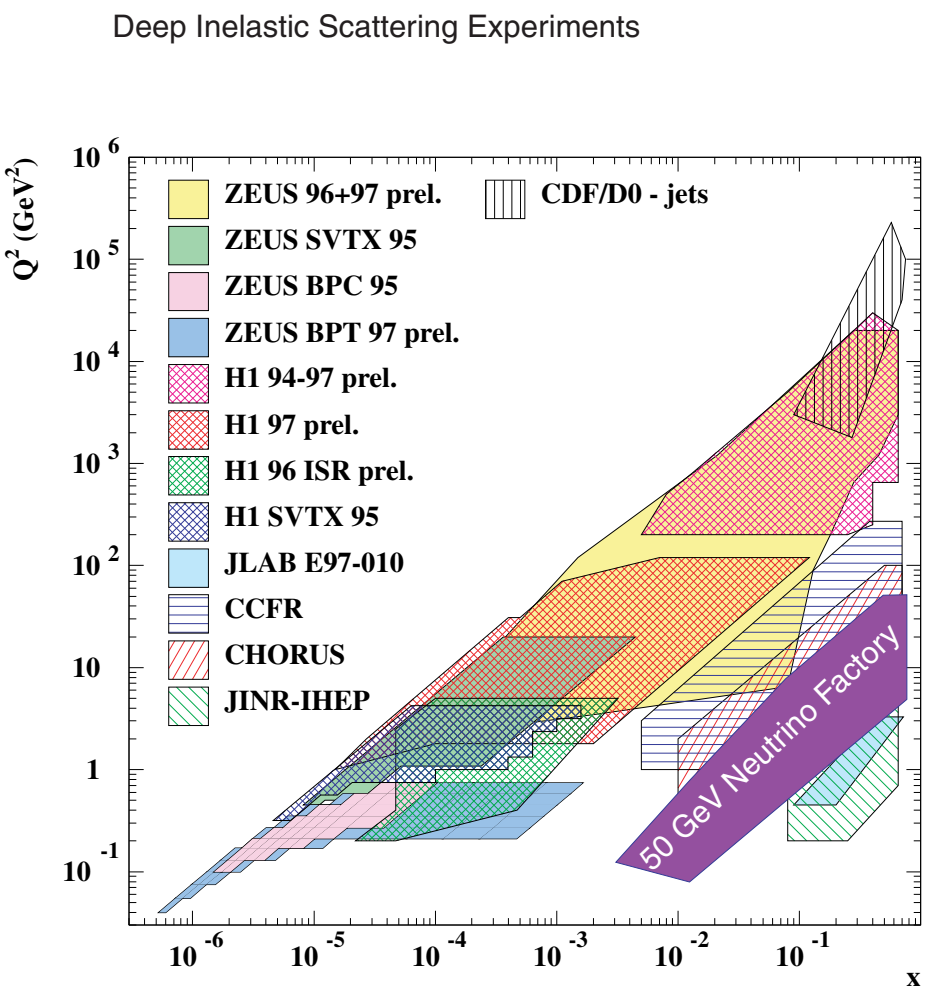

Figure 2: Comparison of kinematic ranges for present DIS experiments with a 50 GeV Neutrino factory.

$$-2y^2F_L(x,Q^2).$$

where M is the mass of the target and the F_i are Structure Functions. $F_L = F_2 - 2xF_1$ is a purely longitudinal structure function. F_3 changes sign for anti-neutrino scattering. There are additional structure functions F_4 and F_5 which are suppressed by factors of the lepton mass squared. For tau and muon neutrino scattering at very low energies, these terms can become quite important.

0.1 Polarized Scattering

If the target is longitudinally polarized with respect to the neutrino polarization, then the cross section difference:

$$\frac{d^2(\sigma^{\leftarrow}_{\Rightarrow} - \sigma^{\leftarrow}_{\Leftarrow})^{\nu(\bar{\nu})}}{dxdy} = \frac{G_F^2 M E_\nu}{\pi}\{\pm y(1 - \frac{y}{2} - \frac{xyM}{2E})xg_1 \mp \frac{x^2yM}{E}g_2 + y^2x(1+\frac{xM}{E})g_3 \quad (7)$$
$$+(1 - y - \frac{xyM}{2E})[(1+\frac{xM}{E})g_4 + g_5]\},$$

is described by two parity conserving Polarized Structure Functions g_1 and g_2, and by three parity violating Polarized Structure Functions g_3, g_4 and g_5. However, if the nucleon is transversely polarized:

$$\frac{d^2(\sigma^{\leftarrow}_{\Uparrow} - \sigma^{\leftarrow}_{\Downarrow})^{\nu(\bar{\nu})}}{dxdy} = \frac{G_F^2 M}{16\pi^2}\sqrt{xyM\,[2(1-y)E - xyM]}\{\mp 2xy(\frac{y}{2}g_1 + g_2) \quad (8)$$
$$+xy^2g_3 + (1 - y - \frac{xyM}{2E})g_4 - \frac{y}{2}g_5\}.$$

is there a factor of 2 missing for the subtraction here

The transverse cross section is suppressed by M/Q with respect to the longitudinal cross section.

0.1.1 Potential structure function measurements at a neutrino factory

In principle, the structure functions can be extracted by fits to the y dependence of the cross section. To date this has proven very difficult as the data must be binned in x, y and Q^2 and no experiment has had sufficient statistics to perform such an analysis with high accuracy[**?**].

Instead, high statistics experiments such as CHARM, CCFR, CDHSW have relied on massive targets (Iron, Calcium) which are approximately isoscalar and have combined neutrino and anti-neutrino information in order to extract average structure functions. The structure functions averages have leading-order parton model interpretations:

$$\overline{F}_2^N(x,Q^2) \simeq \sum(x\mathrm{q}(x,Q^2) + x\overline{\mathrm{q}}(x,Q^2)), \quad (9)$$

$$\overline{F}_3^N(x,Q^2) \simeq \sum(x\mathrm{q}(x,Q^2) - x\overline{\mathrm{q}}(x,Q^2)), \quad (10)$$

where $\overline{F}_2(x,Q^2)$ and $\overline{F}_3(x,Q^2)$ are the average of neutrino and antineutrino structure functions measured on a target which is an average of neutron and proton and $\mathrm{q}(x,Q^2)$ and $\overline{\mathrm{q}}(x,Q^2)$ represent the parton distribution functions or total probability of finding a quark or antiquark in the proton:

$$\mathrm{q}(x,Q^2) = \mathrm{u}(x,Q^2) + \mathrm{d}(x,Q^2) + \mathrm{s}(x,Q^2) + \mathrm{c}(x,Q^2)... \quad (11)$$

$$\overline{\mathrm{q}}(x,Q^2) = \overline{\mathrm{u}}(x,Q^2) + \overline{\mathrm{d}}(x,Q^2) + \overline{\mathrm{s}}(x,Q^2) + \overline{\mathrm{c}}(x,Q^2)... \quad (12)$$

0.1.2 Measurements with high statistics

Given the expectation of 12 M events/year in a 1 m hydrogen or deuterium target at a 50 GeV muon collider we can do a complete analysis of each channel $\nu p, \nu n, \overline{\nu}p, \overline{\nu}n$ without averaging. Such an analysis allows a unique extraction of individual quark flavor parton distribution functions.

Consider νp scattering, a W^+ is exchanged and the reaction can only be sensitive to negatively charged quarks. Due to the helicity dependence of the interaction only left-handed d type and right handed $\overline{\mathrm{u}}$ quarks will be involved.

The leading order parton model cross section is simply

$$\frac{d\sigma^{\nu p}}{dxdy} \simeq \frac{4G_F^2 ME_\nu}{\pi} x[(\mathrm{d}_L(x,Q^2) + \mathrm{s}_L(x,Q^2)) + (\overline{\mathrm{u}}_R(x,Q^2) + \quad (13)$$

$$\overline{\mathrm{c}}_R(x,Q^2))(1-y)^2], \quad (14)$$

and the different contributions can be extracted from the y dependence of this cross section and the corresponding anti-neutrino cross section. The relative s and d contributions can be measured in charm production.

For an unpolarized target $\mathrm{q}_L(x) = \mathrm{q}_R(x) = \frac{1}{2}\mathrm{q}(x)$. For a polarized quark $\mathrm{q}_L(x) = \frac{1}{2}(\mathrm{q}(x) + \delta\mathrm{q}(x))$ and $\mathrm{q}_R(x) = \frac{1}{2}(\mathrm{q}(x) - \delta\mathrm{q}(x))$ where $\delta\mathrm{q}(x)$ is the degree to which the quark spin is aligned with the proton spin[1].

Thus a $\sigma_{\nu p}$ measurement on an unpolarized target can determine $\mathrm{d}+\mathrm{s}$ and $\overline{\mathrm{u}}+\overline{\mathrm{c}}$ by averaging over the proton spin, while by measuring the polarization asymmetry one can measure $\delta\mathrm{d} + \delta\mathrm{s}$ and $\delta\overline{\mathrm{u}} + \delta\overline{\mathrm{c}}$.

Scattering on neutrons can be related to scattering on protons by an isospin transformation which exchanges u and d quarks and anti-quarks. Differences of neutron and proton cross sections can then be used to cancel the u and d components leaving observables sensitive only to s and c distributions.

0.1.3 Perturbative QCD

Neutrinos do not couple directly to gluons. As a result, QCD effects appear in neutrino scattering as well-understood higher order corrections to the leading order parton model. Measurements of the Q^2 dependence of neutrino cross sections are one of the most sensitive measurements of the strong coupling constant α_s and some information on the gluon distribution can be obtained from its coupling to the structure functions via the DGLAP evolution equations. The neutrino structure functions can be divided into two types, singlet and non-singlet, depending on their sensitivity to gluon effects in their evolution.

The structure functions $2xF_1$, F_2 and g_1 are singlet functions and are directly coupled to the gluon distribution via the evolution equations. The structure functions $xF_3 + xF_3$, $2xg_3, g_4$ and g_5 averaged over neutrino and anti-neutrino are non-singlet functions and their evolution is independent of the gluon distribution. The combinations $F_2^p - F_2^n$ and $g_1^p - g_1^n$ also cancel the gluon contributions and are thus non-singlet in nature.

To date, extractions of α_s from non-singlet distributions have been statistics limited and strongly affected by flux uncertainties. The additional factor of 10-100 in statistics and improved flux understanding at a neutrino factory

[1]The traditional Δq spin distributions from electron and muon scattering measure the sum $\Delta\mathrm{q} = \delta\mathrm{q} + \delta\overline{\mathrm{q}}$ as photon probes cannot tell quarks and anti-quarks apart.

should allow vastly improved measurements of strong interaction parameters in this very clean channel.

Once the quark distributions and strong interaction effects have been thoroughly studied in the non-singlet structure function, that knowledge can be used for improved constraints on the gluon distributions via the evolution of the singlet structure functions.

0.2 Nuclear Effects

There is a class of experiments at a neutrino factory which bridges the nuclear and high energy community. This is the study of nuclear effects on the distribution of partons within nuclei relative to protons and deutorons. These nuclear effects have been studied extensively using muon and electron beams but have only been glanced at in low-statistics bubble chamber experiments using neutrinos. If we consider the behavior of the ratio $R_A^{(2)}$ of $F_2(x, Q^2)$ measured on a nucleus (A) to $F_2(x, Q^2)$ measured on a nucleon as a function of x we pass through four distinct regions in going from $x = 0$ to $x = 1.0$:

1. "shadowing" up to $x = 0.1$,
2. "anti-shadowing for $0.1 < x < 0.2$,
3. the "EMC Effect" for $0.2 < x < 0.7$ and
4. "Fermi motion effects" for $x > 0.7$.

Shadowing Region

In the shadowing region there are several effects that should yield a different ratio R_A when using neutrinos as the probe. In the limit $Q^2 \to 0$, the vector current is conserved and goes to 0, however the axial-vector part of the weak current is only partially conserved (PCAC) and $F_2(x, Q^2) \to$ a non-zero constant as $Q^2 \to 0$. According to the Adler theorem [1] the cross section of ν_μ - N can be related to the cross section for π - N at $Q^2 = 0$. What effect does a nuclear environment have on the Adler theorem?

As we increase Q^2 from 0 but keep it under 10 GeV^2 in the shadowing region we enter the region of vector meson dominance (VMD) in μ/e - A scattering. The physics concept of VMD is the dissociation of the virtual boson

into a quark/antiquark pair, one of which interacts strongly with the "surface" nucleons of the target nucleus (thus the "surface" nucleons "shadow" interior nucleons). In ν - A scattering there is an additional contribution from axial-vector mesons that is not present in μ/e - A scattering. Boros et al [2] predict that the resulting shadowing effects in ν - A scattering will be roughly 1/2 that measured in μ/e - A scattering. In a more quantitative analysis, Kulagin [3] used a non-perturbative parton model to predict shadowing effects in ν - A scattering. At 5 GeV^2 he predicts equal or slightly more shadowing in ν - A scattering than in μ/e - A scattering. He also attempts to determine quark flavor dependence of shadowing effects by separately predicting the shadowing observed in $F_2(x,Q^2)$ (sum of all quarks) and $xF_3(x,Q^2)$ (valance quarks only). Fig. 3 shows the results of a 2 year run using predictions of Kulagin's model for F_2 and xF_3. As can be seen, the predicted difference between the shadowing on sea and valence quarks is clearly visible down to $x = 0.02$ - 0.03.

Anti-shadowing Region

Drell-Yan experiments have also measured nuclear effects. Their results are quite similar to DIS experiments in the shadowing region. However, in the anti-shadowing region where R_A makes a brief but statistically significant excursion above 1.0 in DIS, Drell-Yan experiments see no effect. This could be an indication of difference in nuclear effects between valence and sea quarks. Eskola et al [4] quantified this difference by using a leading order/leading twist DGLAP model which used initial nuclear parton distributions from CTEQ4L and GRV-LO and assumed scale evolution of nuclear parton distribution is perturbative. The model predicts that the difference between nuclear effects in $xF_3(x,Q^2)$ and $F_2(x,Q^2)$ persist through the anti-shadowing region as well. Taking the work of Kulagin and Eskola together implies that nuclear effects in $xF_3(x,Q^2)$ should be quite dramatic with more shadowing than $F_2(x,Q^2)$ at lower x and then R_A rising fairly rapidly to yield significant antishadowing around $x = 0.1$. With 14 M events on each target we should be able to measure antishadowing effects and the difference between shadowing effects in $F_2(x,Q^2)$ and $xF_3(x,Q^2)$ to the 6 σ statistical level.

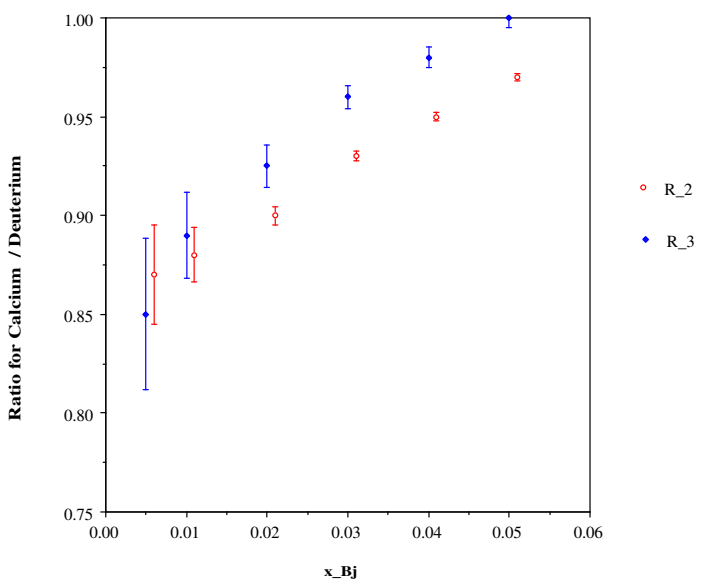

Figure 3: $R_{Ca:D_2}$ for both F_2 and xF_3 as measured with 14 M events on each target.

EMC-effect Region

To determine individual quark contributions to the EMC-effect will be challenging since the participation of sea quarks, and thus the difference between $F_2(x,Q^2)$ and $xF_3(x,Q^2)$, shrinks rapidly with increasing x. However, Eskola's predictions for this region indicate that the contribution of $\overline{u}$ and $\overline{d}$ to $R_A^{(2)}$ in the Q^2 range of this experiment remains well below 1 so that the quantity $R_A^{(2)}$ - $R_A^{(3)}$ should remain negative well into the EMC-effect region.

Behavior of $F_2(x,Q^2)$ as $x \to 1$ in a Nuclear Environment

When working in the "fermi-motion" region it has been shown that we need to add more than the Fermi gas model to a simple nucleon to reproduce the behavior of $F_2(x,Q^2)$ at high x. Few-nucleon-correlation models and multi-quark cluster models allow quarks to have a higher momentum which translates into a high-x tail. In this region $F_2(x,Q^2)$ should behave as e^{-ax}. There have been analysis of this behavior in similar kinematic domains using μ + C and ν + Fe interactions. The muon experiment finds a = 16.5 $\pm$ 0.5 while the neutrino experiment finds a = 8.3 $\pm$ 0.7 $\pm$ 0.7 (systematic). Is the value of a dependent on the nucleus? One would expect any few nucleon correlation or multi-quark effects to have already saturated by Carbon. Is a dependent on the probe?

Summary

There is a very rich program of studying nuclear effects with a neutrino probe in a high statistics neutrino factory experiment. The effects could be measured to statistically significant accuracy in a 2 year exposure to the beam in the near-detector experiment described above. The data gathered would allow separate measurements of the effects on valence quarks and sea quarks across much of the x range.

The nuclear community should be informed of what a valuable tool for nuclear research awaits them in the neutrino factory facility.

0.3 Spin Structure

The relation between the polarized neutrino cross sections and the structure functions $g_1 - g_5$ was given in equations 8 and **??**

In the naive parton model,

$$g_1^{\nu p}(x,Q^2) = \delta \mathrm{d}(x,Q^2) + \delta \mathrm{s}(x,Q^2) + \delta \overline{\mathrm{u}}(x,Q^2) + \delta \overline{\mathrm{c}}(x,Q^2), \quad (15)$$

$$g_1^{\bar{\nu} p}(x,Q^2) = \delta \mathrm{u}(x,Q^2) + \delta \mathrm{c}(x,Q^2) + \delta \overline{\mathrm{d}}(x,Q^2) + \delta \overline{\mathrm{s}}(x,Q^2). \quad (16)$$

g_2 has a a twist–2 (g_2^{WW}) and a twist–3 ($\bar{g}_2$) contribution and has no simple parton model interpretation,

$$g_2 = g_2^{WW} + \bar{g}_2 \quad (17)$$

$$g_2^{WW}(x,Q^2) = -g_1(x,Q^2) + \int_x^1 \frac{dy}{y} g_1(y,Q^2). \quad (18)$$

For g_3 and $g_4 + g_5$ the parton model predictions are:

$$g_{4+5}^{\nu p}(x,Q^2) = 2x g_3^{\nu p}(x,Q^2) \quad (19)$$
$$= -x[\delta d(x,Q^2) + \delta s(x,Q^2) - \delta \overline{\mathrm{u}}(x,Q^2) - \delta \overline{\mathrm{c}}(x,Q^2)],$$

$$g_{4+5}^{\bar{\nu} p}(x,Q^2) = 2x g_3^{\bar{\nu} p}(x,Q^2) \quad (20)$$
$$= -x[\delta u(x,Q^2) + \delta c(x,Q^2) - \delta \overline{\mathrm{d}}(x,Q^2) - \delta \overline{\mathrm{s}}(x,Q^2)].$$

A high intensity neutrino factory should be able to answer many unresolved questions about the spin structure of the nucleon. The nucleon spin ($\frac{1}{2}$) can decomposed in terms of quarks and gluon contributions:

$$\frac{1}{2} = \frac{1}{2}\Delta\Sigma + \Delta g + L_q + L_g, \quad (21)$$

where $\Delta\Sigma\Delta u + \Delta d + \Delta s + \Delta c$ is the net quark helicity and Δg is the net gluon helicity along the nucleon spin direction, while L_i are their relative orbital angular momentum.(We use Δq as a shorthand for the integral $\Delta \mathrm{q}(x)dx$.)

To date, the only experiments which address this question are low energy charged lepton polarized deep-inelastic scattering experiments (PDIS) where only the parity conserving polarized structure functions g_1^l and g_2^l can be measured.

g_1^ℓ can be written in the leading order parton model as a sum of a nonsinglet and singlet part:

$$\begin{aligned} g_1^\ell(x,Q^2) &= g_{1,NS}^\ell(x,Q^2) + g_{1,S}^\ell(x,Q^2) && (22)\\ &= \frac{1}{2}\sum(e_i^2 - < e^2 >)\Delta \mathrm{q}_i(x,Q^2) + \frac{1}{2}\sum < e^2 > \Delta \mathrm{q}_i(x,Q^2) && (23)\\ & && (24) \end{aligned}$$

The first non-singlet term evolves independently of the gluonic spin contribution while the second is coupled to, and thus depends on the gluon spin contribution Δg.

In integral

$$\begin{aligned} \Gamma_1^\ell(Q^2) &= \int dx g_1^{lp/n}(x,Q^2) && (25)\\ &= \Gamma_{1,NS}^\ell(Q^2) + \Gamma_{1,S}^\ell(Q^2) && (26)\\ \Gamma_1^{\ell p}(Q^2) &= \frac{C_1^{NS}(Q^2)}{6}\Big[\frac{1}{2}a_3 + \frac{1}{6}a_8\Big] + \frac{C_1^S}{9}a_0 && (27)\\ \Gamma_1^{\ell n}(Q^2) &= \frac{C_1^{NS}(Q^2)}{6}\Big[-\frac{1}{2}a_3 + \frac{1}{6}a_8\Big] + \frac{C_1^S}{9}a_0 && (28)\\ & && (29) \end{aligned}$$

Where the C_1 are coefficient functions and the axial charge matrix elements

$$\begin{aligned} a_3 &\equiv F + D \simeq \Delta\mathrm{u} - \Delta\mathrm{d} && (30)\\ a_8 &\equiv 3F - D \simeq \Delta\mathrm{u} + \Delta\mathrm{d} - 2\Delta\mathrm{s} && (31)\\ a_0 &\equiv \Delta\mathrm{u} + \Delta\mathrm{d} + \Delta\mathrm{s} = \Delta\Sigma && (32)\\ & && (33) \end{aligned}$$

can be expressed in terms of coupling constants F and D obtained from neutron and hyperon beta decays [**?**]. Because the interaction between Δg and $\Delta\Sigma$ in the evolution of the singlet (a_0) component, interpretation of Γ_1^ℓ in terms of the quark spin is problematic. Figure shows NLO QCD predictions for $\Delta\Sigma$ as a function of Δg.

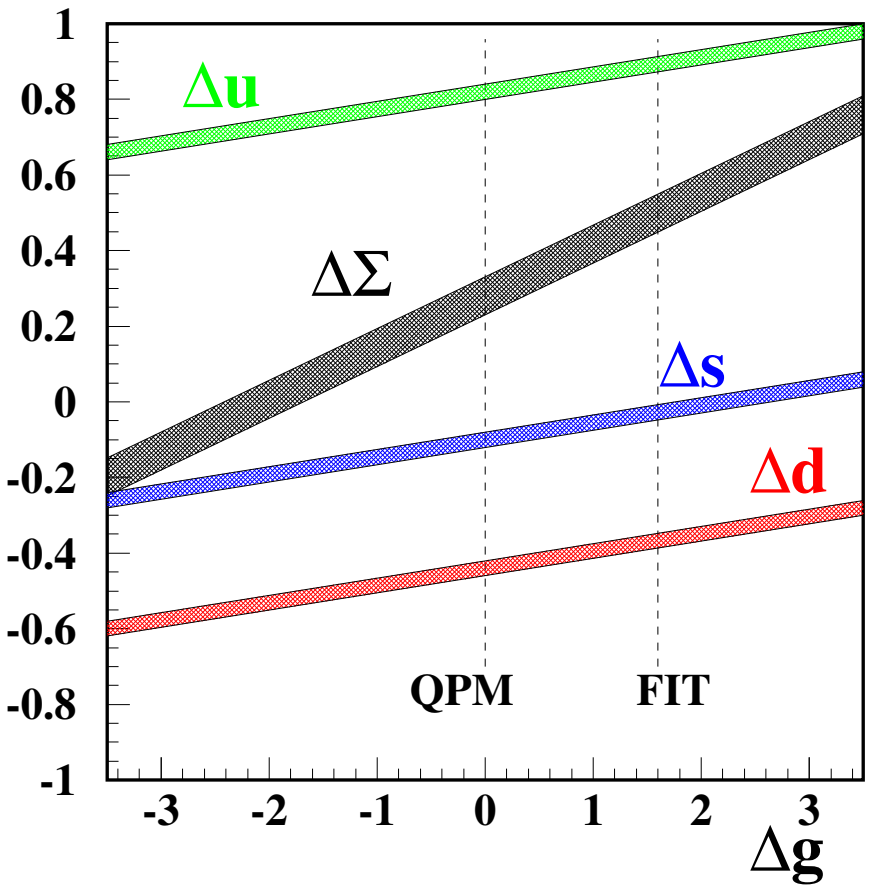

Figure 4: Model dependent decomposition of singlet term into quarks and gluon based on PDIS data, $a_0 \to \Delta q - 3\frac{\alpha_s}{2\pi}\Delta g$. The QPM expectation and the results from a NLO fit of the Q^2 evolution of most of the available data on g_1^l are also shown. From the fit it was found that under this singlet the error is dominated by theoretical uncertainties.

Neutrino beams introduce both additional parity violating spin structure functions $g_3, g_4 and g_5$ and new combinations based on sums and differences of neutrino and anti-neutrino scattering. For example the sum

$$\Gamma_1^\nu + \Gamma_1^\nu = \int dx(g_1^\nu + g_1^{\overline{\nu}})$$

for both proton and neutron targets is only sensitive to the singlet a_0 term and no input from beta decay is necessary.

On a deuterium target, the u and d contributions to g_3 can be cancelled leading to a direct measurement of the strange sea contribution to the nucleon spin

$$g_3^{\nu(np)} - g_3^{\overline{\nu}(np)} = -2(\delta \mathrm{s} + \delta \overline{\mathrm{s}}) + 2(\delta \mathrm{c} + \delta \overline{\mathrm{c}})$$

.

which can also be studied via polarization asymmetries in charm production from strange quarks.

The structure functions $g_3 - - g_5$, like F_3 are non-singlet functions in which contribution from gluons cancel. Comparison of the non-singlet functions with the single functions g_1 and F_2 is an indirect way of measuring the contribution of gluons Δg.

1 Experimental Setup at the Neutrino Factory

An ideal polarized target will be one that has a mass of at least 10 kg, high polarization, large fraction of polarizable material, f and has the capability of having both protons and neutron polarized which is required to study the 'sea quark' contribution to the nucleon spin. 'ICE' targets are a new technology which looks very promising.'ICE' is a HD solid polarizable compound material. Both the H and the D can be polarized, separately or simultaneously. The expected polarization and dilution are P_H=80%, and $f_H = 1/3$ for H, and P_D=50% and $f_D = 2/3$ for deuteron. A 7 kg (ρ_t=1.1gr/cm^2) polarized target with the qualities mentioned above can be built out of an ICE-target (20 cm in radius, 50 cm thick) mounted in the detector proposed for structure functions studies. Raw event rates in such a detector would be around 20M per 10^{20} muon decays.

In order to measure g_1 both ν and $\overline{\nu}$ beams are needed. A double spin difference with longitudinally polarized nucleon and evaluated eq. is measured:

$$A_{g_1} = \{\sigma_{\uparrow\uparrow} - \sigma_{\uparrow\downarrow}\}_{\nu} - \{\sigma_{\uparrow\uparrow} - \sigma_{\uparrow\downarrow}\}_{\overline{\nu}}. \tag{34}$$

This difference should be measured not only as a function of x but also as a function of y in order to see the effect of different suppression factors of unwanted structure functions like g_2. Similarly, for g_3 we evaluate $A_{g_3} = \{\sigma_{\uparrow\uparrow} - \sigma_{\uparrow\downarrow}\}_{\nu} + \{\sigma_{\uparrow\uparrow} - \sigma_{\uparrow\downarrow}\}_{\overline{\nu}}$. Cross checks can be made with the target transversely polarized where the suppression factors for the different structure functions are different.

Analysis of the double difference can be done in 10-bins in x, if the acceptance for events is $> 40\%$ then the error on the asymmetry in each x bin would be: $\delta A_{g_1} \simeq (f P_T \sqrt{N})^{-1} \sim 1\%$.

Conclusion

If the neutrino beam intensities and polarized target described above are feasible, the physics motivations would be very strong. We will be able to do measurements where we can cleanly separate singlet (gluon-dependent) from non-singlet (gluon-free) terms. Furthermore, due to the nature of the neutrino charged interactions it will be possibility to perform a measurement of the polarization of the proton's quarks by flavor, with sea and valence contributions separated.

1.1 Charm Production and $D^0 - \overline{D}^0$ Mixing

Neutrino interactions are a very good source of clean, sign-tagged charm particles. Single charm quarks are produced via the processes

$$\begin{aligned}
\nu \mathrm{s} &\rightarrow \ell^- \mathrm{c} \quad \text{Cabbibo favored} && (35)\\
\nu \mathrm{d} &\rightarrow \ell^- \mathrm{c} \quad \text{Cabbibo suppressed} && (36)\\
\nu \overline{\mathrm{s}} &\rightarrow \ell^+ \overline{\mathrm{c}} \quad \text{Cabbibo favored} && (37)\\
\nu \overline{\mathrm{d}} &\rightarrow \ell^+ \overline{\mathrm{c}} \quad \text{Cabbibo suppressed} && (38)\\
& && (39)
\end{aligned}$$

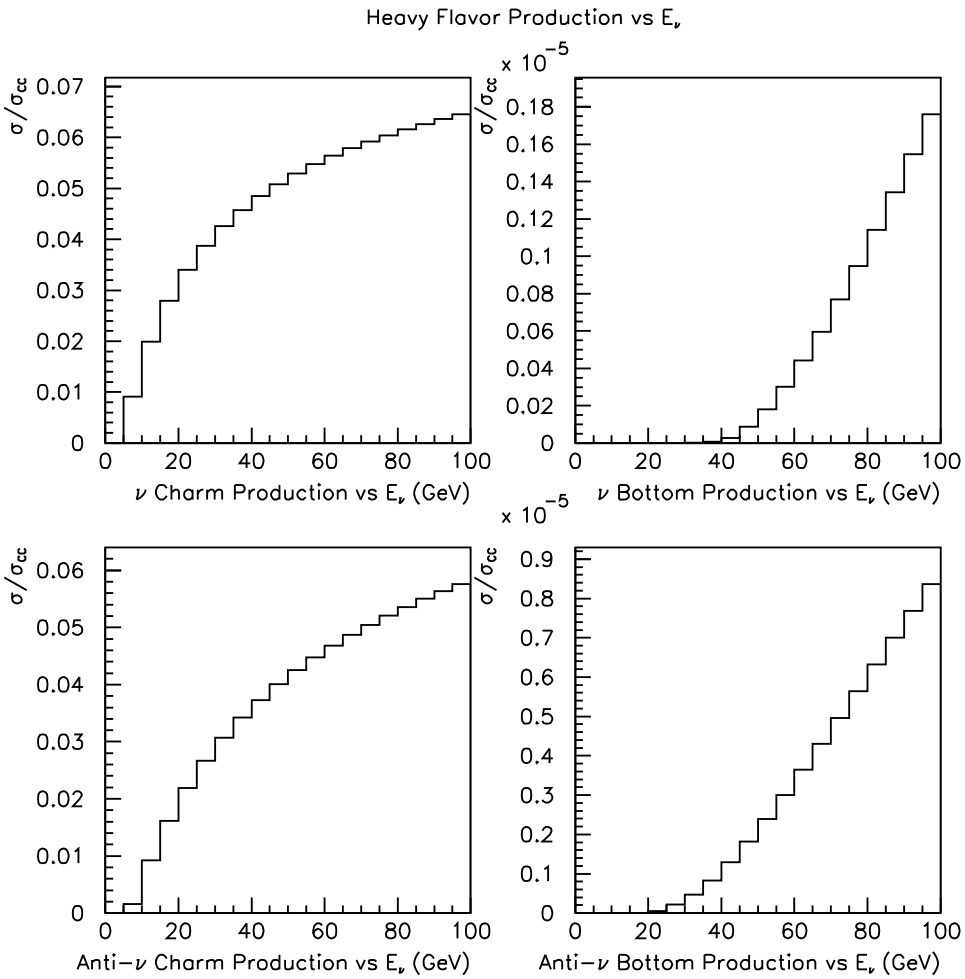

Figure 5: Charm and bottom quark production as a fraction of the total cross-section as a function of E_ν.

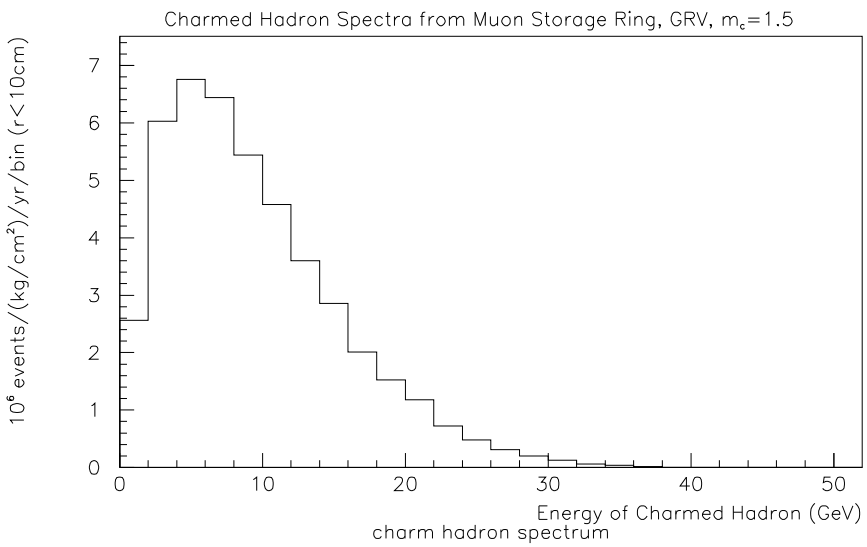

Figure 6: Charmed hadron spectra from neutrino interactions in a near detector from a 50 GeV muon storage ring.

The fraction of heavy flavor produced as a function of E_ν is shown in Figure 5. As shown from the charmed hadron spectrum in Figure 6, a sample of 3×10^9 charged-current DIS interactions from a 50 GeV muon beam will include 10^7 charmed hadrons above 20 GeV, 6×10^7 above 10 GeV and 12×10^7 above 4 GeV. Furthermore, all of these charmed hadrons are flavor tagged at the point of production by the charge of the outgoing primary lepton (c production with ℓ^- and $\overline{c}$ production with ℓ^+).

There are several interesting physics motivations for charm studies at a muon storage rings, including measurements of the strange contribution to proton structure and spin; however, the primary motivation for producing charm by this method is the cleanliness of the final state relative to hadroproduction and the flavor tagging in production. This experimental fact compliments the theoretically "clean laboratory" of charm in searches for FCNC, CP asymmetries and $\mathrm{D}^0 \to \overline{\mathrm{D}^0}$ oscillations, all of which are very small in the standard model because of the lack of coupling of charm to the heavy top quark.

As an example of the physics reach of a neutrino charm factory, consider the example of $D^0 - \overline{D^0}$ mixing measurements. The most sensitive current searches for time-integrated mixing place limits on the process of $\sim 5 \times 10^{-3}$ [10, 11]. BaBar expects to have sensitivity to mixing at the $\sim 5 \times 10^{-4}$ level after several years at design luminosity [12]. These measurements are ultimately limited by tagging mistakes and backgrounds to final state D^0 or $\overline{D^0}$ identification from doubly-Cabibbo suppressed decays, such as $D^0 \to K^+\pi^-$ which occur at the few part per thousand level.

At a 50 GeV muon storage ring, with a high mass detector, one could probe $D^0 - \overline{D^0}$ mixing *via*

$$\begin{aligned} \nu N \to \quad & c\ell^- X \\ & \hookrightarrow \ell^+ X \\ & \hookrightarrow \overline{c} \to \ell^- X, \end{aligned}$$

and its charge conjugates. The appearance of like-signed leptons would indicate mixing, where opposite-signed leptons are expected. An experiment at a 50 GeV muon storage ring with a one ton (fiducial) target made up of silicon strip detectors interleaved with heavier material would observe $\approx 3 \times 10^9$ muon-neutrino charged-current interactions. Assuming 50% of the charm produces hadronizes as a D^0 or $\overline{D^0}$, this would result in the observation of

210^6 tagged neutral charm meson semi-leptonic decays in either the muon or electron channel.

Precision Electroweak Measurements

Introduction

Precision measurements of electroweak parameters from neutrino experiments have played an important role in testing the Standard Model and in searching for new physics. Even with the wealth of on-shell W and Z bosons today at colliders, the neutrino data remains important and is complimentary to collider studies. The intense flux of neutrinos from a neutrino factory opens up a whole new era of precision electroweak measurements that were previously limited by statistics.

Three interesting precision measurements can be contemplated at a neutrino factory facility, and each can be cast as a precision measurement of the weak mixing angle, $\sin^2\theta_W$. The experiment that most dramatically highlights new capabilities at a neutrino factory is the study of neutrino-electron cross sections. The second possible experiment is the extraction of $\sin^2\theta_W$ from the neutral-current to charged-current deep inelastic scattering (DIS) cross-sections, a measurement which currently is the most precise test of weak interactions in neutrinos and which is currently limited by statistics[14], although difficult theoretical systematics are not far behind. A final possibility is the study of weak boson scattering from photons in the so-called neutrino "trident" process.

Only the first two possibilities are discussed here in detail. Trident processes are not considered here because of the difficult theoretical systematics that will ultimately limit the measurements[15].

Neutrino-Electron Scattering

Neutrino-electron elastic scattering,

$$\nu e^- \to \nu e^-, \tag{40}$$

is perhaps the most promising reaction for the precise probe of electroweak unification from neutrino interactions. Because the target is point-like, its

structure does not introduce uncertainties in extracting parameters of the electroweak interaction from observed cross-sections. These measurements will therefore be limited only by statisticaland experimental uncertainties. The best previous measurements of νe scattering come from the CHARM II experiment which observed approximately 5000 events [16].

Two distinct measurements are possible at a muon storage ring because neutrino-electron scattering includes different diagrams for the beams from positive and negative muons. The processes in the $\nu_\mu\overline{\nu_e}$ and $\overline{\nu_\mu}\nu_e$ beams are

$$\begin{aligned} \bar{\nu}_\mu e^- &\to \bar{\nu}_\mu e^-, \quad \nu_e e^- \to \nu_e e^-, \\ \nu_\mu e^- &\to \nu_\mu e^-, \quad \bar{\nu}_e e^- \to \bar{\nu}_e e^-, \end{aligned} \tag{41}$$

where the electron-neutrino and electron-antineutrino scattering process includes a charged-current ($W^\pm$ exchange) in the t-channel and s-channel, respectively. The differential cross-section with respect to $y = E_e/E_\nu$ is given by

$$\frac{d\sigma(\nu e^- \to \nu e^-)}{dy} = \frac{2G_F^2 m_e E_\nu}{\pi}\left[g_L^2 + g_R^2(1-y)^2\right], \tag{42}$$

where terms of $\mathcal{O}(m_e/E_\nu)$ are neglected and expressions for the left-handed and right-handed coupling constants, g_L and g_R, for each of the processes in shown in equation 41 are given in Table 2. The numerical values for the cross-sections after integrating over y are:

$$\sigma(\nu e^- \to \nu e^-) = 1.6 \times 10^{-41} \times E_\nu[GeV] \times \left[g_L^2 + \frac{1}{3}g_R^2\right], \tag{43}$$

where the values for the final term are also given in Table 2. Note that neutrino-electron scattering has a much lower cross-section than DIS, roughly down by the ratio of m_e to m_p. Experimentally, it should be noted that the observed neutrino-electron scattering rate will be summed over both beams since the observed final states are identical.

The experimental signature for $\nu - e$ scattering is a single negatively charged electron with a small transverse momentum relative to the incoming neutrino,

$$p_t^{\nu_\ell} < \sqrt{2m_e E_\nu}. \tag{44}$$

The normalization mode is the appearance of a single muon with similarly low p_t. Of course, the neutrino beam itself has a characteristic divergence

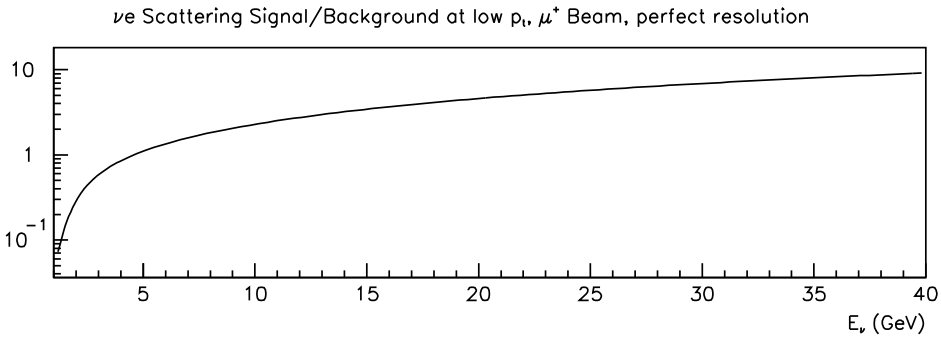

Figure 7: Signal to noise in the low p_t region ($p_t^2 < \frac{\pi^2}{16\gamma_\mu^2} + \frac{m_e E_\nu}{2}$) as a function of E_ν.

from decay kinematics of $\frac{\pi}{4\gamma_\mu}$, and therefore the observed lepton p_t relative to the mean beam direction is given by

$$\left\langle p_t^\ell \right\rangle \approx \sqrt{\frac{\pi^2}{16\gamma_\mu^2} + \frac{m_e E_\nu}{2}}. \tag{45}$$

For a 50 GeV storage ring, this factor is dominated by the fundamental p_t of the interaction and is typically ~ 90 MeV. For a lower energy storage ring of about 15 GeV, these factors become equal.

The primary background to this measurement is from quasi-elastic $\nu_e - N$ or $\bar{\nu}_e - N$ scattering events which occur at p_t up to $\sqrt{m_N E_\nu}$ and form a smooth background underneath the signal in p_t. Figure 7 shows the estimated signal to background ratios expected in the low p_t region.

The detector design must therefore be capable of resolving the p_t of an electron (but not necessarily the charge) to a scale significantly below the background at $\langle p_t \rangle \approx \sqrt{\frac{1}{2} m_p E_\nu}$, which corresponds to electron angles of

$$\theta_e \sim \sqrt{\frac{m_p}{2E_\nu}}. \tag{46}$$

This favors the use of a fully active, high resolution tracking detector with sub-radiation length sampling in order to resolve the p_t of the single electron before it is significantly broadened by shower development. A liquid Argon TPC, such as the one proposed for the ICANOE experiment[17]

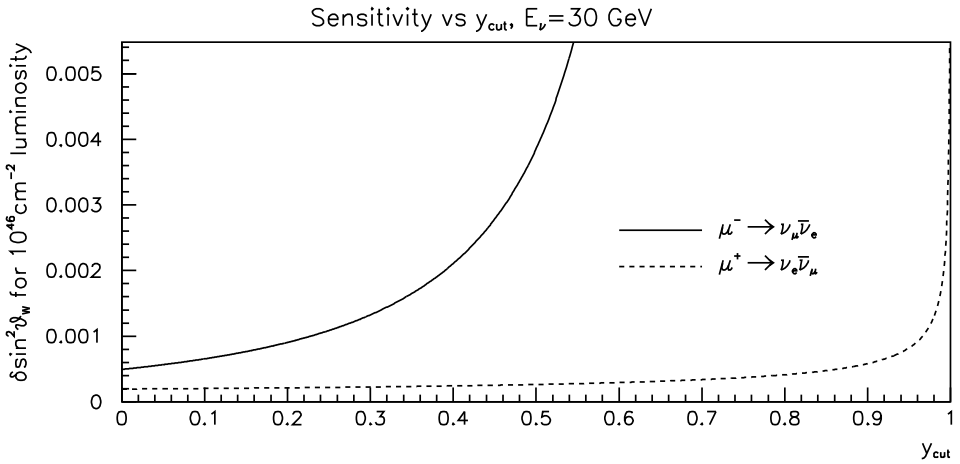

Figure 8: Statistical uncertainty in $\sin^2\theta_W$ for a luminosity of 10^{46} cm^{-2} as a function of $y_{\rm cut}$ for a 30 GeV neutrino beam. Note that the μ^- produced beam is much less sensitive to $\sin^2\theta_W$ due to nearly exactly cancellation in the $\sin^2\theta_W$ dependence of the two neutrino species in the beam.

might be ideal for such a measurement. Other possibilities are a scintillating fiber/tungsten calorimeter.

The largest experimental challenge for measurement is likely to be the normalization of the absolute neutrino flux. Despite the precise knowledge of muon decays, it would be extremely difficult to predict the precise neutrino flux at the 10^{-4} level merely from monitoring the parent muon beam. Instead, the signal processes will probably have to be normalized to the theoretically predictable processes of inverse muon decay, $\nu_\mu e^- \to \nu_e \mu^-$, and muon production through annihilation, $\overline{\nu}_e e^- \to \overline{\nu}_\mu \mu^-$, both of which occur only in the $\nu_\mu\overline{\nu_e}$ beam. Normalization of the ν_e beam may be possible through comparison neutrino-nucleon scattering, $\nu N \to l^\pm N'$, in the $\overline{\nu_\mu}\nu_e$ and $\nu_\mu\overline{\nu_e}$ beam.

for a 20 ton detector at a 50 GeV muon storage ring, with 2×10^{20} μ^- decays/year there will be approximately 1.5×10^{10} DIS charged current events and 8.5M $\nu_\mu/antinue$-electron scatters per year. These lead to an estimated sensitivity of $\delta\sin^2\theta_W^{(\rm stat)} \sim 0.0002$

Neutrino-Nucleon Scattering

There were two dominant systematic uncertainties in present-day meaurements of the weak mixing angle in neutrino nucleon scatering, ν_e contamination in the ν_μ beam and the kinematic suppression of scattering from strange quarks in the charged current channel.

For an isoscalar target, the neutral current rates can be related to the charged current rates via [**?**]:

$$R_\nu - \Delta R_s = (\frac{1}{2} - \sin^2\theta_W + \frac{5}{9}\sin^4\theta_W)[1 - \Delta R_c] + \frac{5}{9}\sin^4\theta_W[r - r\Delta\overline{R}_c] \quad (47)$$

$$R_{\overline{\nu}} - \Delta\overline{R}_s = (\frac{1}{2} - \sin^2\theta_W + \frac{5}{9}\sin^4\theta_W)[1 - \Delta\overline{R}_c] + \frac{5}{9}\sin^4\theta_W[\frac{1}{r} - \frac{1}{r}\Delta R_c] \quad (48)$$

where $R_{\nu/\overline{\nu}}$ is the ratio of neutral to charged current cross sections, $r \sim 0.5$ is the ratio of charged current anti-neutrino to neutrino cross sections and ΔR_s and ΔR_c are small corrections for the kinematic suppression of s $\to$ c in charged current scattering where the neutral current process s $\to$ s has no suppression. The charm corrections can be eliminated by a judicious subtraction of neutrino and anti-neutrino rates [**?**] but with a consequent reduction in statistical power.

Experiments CITE(CDHSW, CCFR, NUTEV) to date have had integrated fluxes of 10^{15}-10^{16} neutrinos and have relied on dense iron targets. In such targets neutral current events are distinguished from charged current events by the presence or absence of a muon in the final state. But in a calorimeter, electron neutrino charged current induced events will be look very similar to neutral current events and form a significant background for precision measurements with conventional beams produced by pion and kaon decay.

The most precise measurement to date is from the NuTeV collaboration [23] of

$$\sin^2\theta_W = 0.2253 \pm 0.0019(stat) \pm 0.0010(syst). \quad (49)$$

At a neutrino factory, the neutrino flux will be several orders of magnitude higher but the beam will consist of approximately equal numbers of ν_μ and $\overline{\nu}_e$. This makes a detector capable of distinguishing electron charged current events from neutral current events desirable and implies a low density detector such as those considered for the deep-inelastic scattering studies.

We have considered several possible observables for a neutrino factory measurement and propose:

$$R_e^{\mu^-} = \frac{\sigma(\nu_\mu, NC) + \sigma(\overline{\nu}_e, NC)}{\sigma(\nu_\mu, CC) - \sigma(\overline{\nu}_e, CC)} = \frac{R^\nu + grR^{\overline{\nu}}}{1 - gr} \quad (50)$$

or

$$\hat{R}^{\mu^-} = \frac{\sigma(\nu_\mu, NC) + \sigma(\overline{\nu}_e, NC) + \sigma(\overline{\nu}_e, CC)}{\sigma(\nu_\mu, CC)} = R^\nu + grR^{\overline{\nu}} + gr \quad (51)$$

for the $\nu_\mu\overline{\nu_e}$ beam, and

$$R_e^{\mu^+} = \frac{\sigma(\overline{\nu}_\mu, NC) + \sigma(\nu_e, NC)}{\sigma(\nu_e, CC) - \sigma(\overline{\nu}_\mu, CC)} = \frac{R^\nu + g^{-1}rR^{\overline{\nu}}}{1 - g^{-1}r} \quad (52)$$

or

$$\hat{R}^{\mu^+} = \frac{\sigma(\overline{\nu}_\mu, NC) + \sigma(\nu_e, NC) + \sigma(\nu_e), CC)}{\sigma(\overline{\nu}_\mu, CC)} \quad (53)$$

$$= \frac{g}{r}R^\nu + R^{\overline{\nu}} + \frac{g}{r} \quad (54)$$

for the $\overline{\nu_\mu}\nu_e$ beam, where $R_{\nu/\overline{\nu}}$ is the ratio of neutral to charged current cross sections from equation 47. The variable g is the energy-weighted flux ratio between ν_μ and $\overline{\nu}_e$ or, equivalently, between $\overline{\nu}_\mu$ and ν_e:

The observable R_e^μ require electron identification while $\hat{R}^\mu$ requires only muon identification.

The flux ratio for neutrinos and anti-neutrinos g is:

$$g \equiv \frac{\int \Phi(E_{\overline{\nu}_e}) E_{\overline{\nu}_e} dE_{\overline{\nu}_e}}{\int \Phi(E_{\nu_\mu}) E_{\nu_\mu} dE_{\nu_\mu}} = \frac{\int \Phi(E_{\nu_e}) E_{\nu_e} dE_{\nu_e}}{\int \Phi(E_{\overline{\nu}_\mu}) E_{\overline{\nu}_\mu} dE_{\overline{\nu}_\mu}} \simeq \frac{6}{7}. \quad (55)$$

Due to the nature of muon decay kinematics, the flux ratio should be quite well known. However, the relative detection efficiencies for muons and electrons must be known at the 2×10^{-4} level in order to determine $\sin^2\theta_W$ to 10^{-3} by the first method. In addition, the charm contributions are not

cancelled in this observable and must be measured directly in the same experiment.

For the R_e measurement, which requires electron identification, an active target of 20cm radius, 10 gr/cm^2 thick consisting of either CCD's or silicon strip detectors ($\sim$ 140 300-μm detectors) spaced over a meter and followed by the tracking, electromagnetic and hadron calorimetry and muon identification proposed above for structure function measurements would yield 15M muon and 8M electron charged current deep-inelastic scattering events/10^{20} μ^- decays and would yield a statistical precision of 0.0004 in $\sin^2\theta_W$. The charm corrections partially cancel in this observable and would also be measured directly via the 2M charm events/year produced in such a detector.

The $\hat{R}$ measurement, which relies only on muon identification can be done with a much denser target, perhaps an iron/silicon sandwich calorimeter. Such a calorimeter 200 gr/cm^2 thick would have a statistical sensitivity of$\Delta \sin^2\theta_W$ 0.0001 per year at a 50 GeV machine. This method is quite similar to the method used in the NuTeV **??** measurement and would be dominated by systematic errors.

Heavy Lepton Mixing

A muon storage ring offers ample opportunities to search for new phenomena in yet unexplored physical regions. One such opportunity is the ability to search for the existence of neutral heavy leptons. Several models describe heavy isosinglets that interact and decay by mixing with their lighter neutrino counterparts [33, 39]. The high intensity neutrino beam created by the muon storage ring provides an ideal setting to search for neutral heavy leptons with a mass below the muon mass, 105.6 MeV/c^2.

It is postulated that neutral heavy leptons (L_0) could be produced from muon decay when one of the neutrinos mixes with its heavy, isosinglet partner. Neutral heavy leptons can be produced via one of two channels:

$$\mu^- \rightarrow L_0 + \overline{\nu}_e + e^- \tag{56}$$

$$\mu^- \rightarrow \nu_\mu + L_0 + e^- \tag{57}$$

The branching ratio for each of these reactions is given by:

$$BR(\mu \to L_0 \mu e) = |U_i|^2 (1 - 8x_m^2 + 8x_m^6 - x_m^8 + 12x_m^4 \ln x_m^2) \qquad (58)$$

Here $x_m \equiv m_{L_0}/m_\mu$ and $|U_i|^2$ is the mixing constant between the specific type of neutrino and the neutral heavy lepton: $U_i \equiv \langle L_0 | \nu_i \rangle$. Note that $|U_\mu|^2$ and $|U_e|^2$ need not be identical.

Once produced, a neutral heavy lepton of such low mass will either decay via $L_0 \to \nu\nu\nu$, $L_0 \to \nu ee$, or $L_0 \to \gamma\nu$. The most viable mode for detection is the two-electron channel. For this particular decay mode, the L_0 can decay either via charged current or charged and neutral current interactions. The branching ratio for this decay process has been previously calculated [35]. Since the decay width is proportional to U_j^2, the number of L_0's detectable is proportional to $U_i^2 * U_j^2$ in the limit where the distance from the source to the detector is short compared to the lifetime of the L_0.

Using the above model, one can estimate the number of neutral heavy leptons produced at the muon storage ring which later decay within a given detector. The number of detected neutral heavy leptons is given by the equation below:

$$N_{L_0} = N_\nu * BR(\mu \to L_0 \nu e) * \epsilon * e^{-L/\gamma c\tau} * BR(L_0 \to detectable) * (1 - e^{-\delta l/\gamma c\tau}) \qquad (59)$$

Here N_ν is the number of neutrinos produced from muon decay, $BR(\mu \to L_0 \nu e)$ is the branching ratio of muons decaying into neutral heavy leptons versus ordinary muon decay, L is the distance from the beamline to the detector, δl is the length of the detector, ϵ is the combined detector and geometric efficiency, τ is the L_0 lifetime, and $BR(L_0 \to detectable)$ is the branching ratio for the neutral heavy lepton decaying via a detectable channel (presumably $L_0 \to \nu ee$).

In testing the sensitivity to L_0 production at the muon storage ring, we make a few underlying assumptions. We assume that the storage ring utilizes a pure, unpolarized muon beam with straight sections such that 25 percent of the muons will decay to neutrinos pointing towards the detector. We assume that the fiducial volume is 3 meters in diameter and 30 meters in length, and that the detector has sufficient tracking resolution to detect the e^+e^- vertex from the L_0 decay. We assume for now that the background is negligible. These parameters correspond to the fiducial volume of the decay channel used for the L_0 search at E815 (NuTeV) [36, 37].

The sensitivity of the detector has been calculated for a number of different muon energies and beam intensities. Figure 9 shows limits on the L_0-ν_μ mixing as a function of L_0 mass. One achieves the best limits from using relatively low energy/high intensity muon beams. This is a major improvement over previous neutral heavy lepton searches, where limits do not reach below $6.0 * 10^{-6}$ in the low mass region [38, 39].

The single event sensitivity quoted here depends greatly on having minimal background levels in the signal region. Part of this can be achieved by kinematic cuts which discriminate against neutrino interactions in the detector material. However, it will probably be necessary to reduce the amount of material in the fiducial region greatly compared to NuTeV. We estimate that even if the decay region is composed only of helium gas, the number of neutrino interactions will approach a few thousand. The ideal detector, therefore, would consist of a long vacuum or quasi-vacuum pipe with appropriate segmentation for tracking. The decay pipe could be used in conjunction with larger neutrino detectors adapted for the muon storage ring.

The muon storage ring may prove to be an ideal location to continue the search for neutral heavy leptons. The high intensity neutrino beam allows for a neutral heavy lepton search to be sensitive to the 10 – 100 MeV/c^2 mass range. In addition, such a neutral heavy lepton program could easily interface with a neutrino detector which uses the same neutrino beam. It is also clear, however, that a neutral heavy lepton search would receive the most benefit at lower muon energies, and thus would yield best results at the earlier stages of the muon storage ring program.

2 Neutrino Magnetic Moments

Although neutrino oscillation searches focus on the mass differences between neutrino eigenstates, neutrinos can possess other observable properties such as a magnetic moment. A measurement of the neutrino magnetic moment (NMM) would not only have great impact in the field of cosmology, particularly the development of stellar models, but would also help constrain several Standard Model extensions. An important experimental advantage is that a NMM search can run parasitically as the front–end to a typical long baseline detector.

Despite their lack of charge, a neutrino can possess a non-zero magnetic

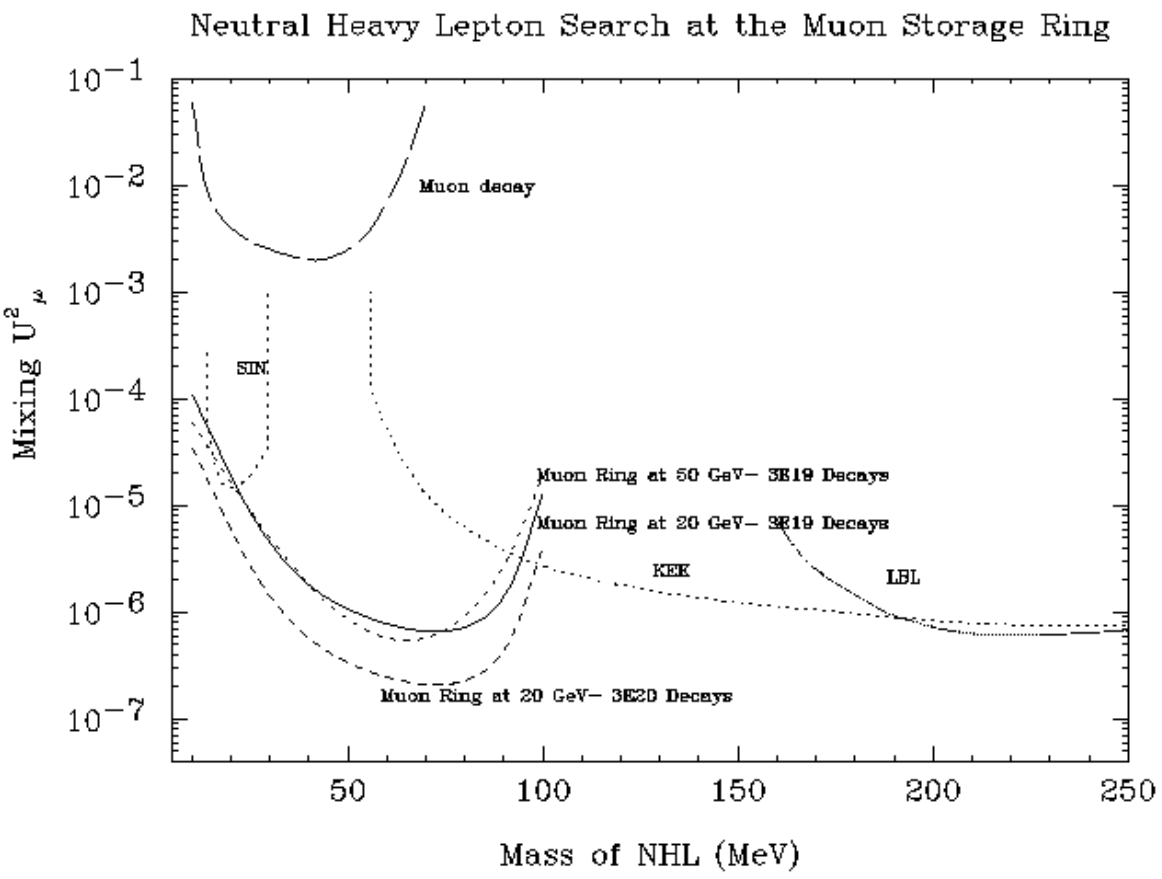

Figure 9: Limits on $|U_{\mu L}|^2$ as a function of L_0 mass for one year of running. The curves show sensitivities for 20 GeV and 50 GeV muon energies. Sensitivities assume no background events in signal region.

moment that can arise through loop diagrams. In the Standard Model, extended to include a right–handed neutrino or with left–handed neutrinos which have mass, the expected [40] neutrino magnetic moment magnitude is given by

$$\mu_\nu \simeq 3 \times 10^{-19}\ \mu_{Bohr} \cdot (\frac{m_\nu}{1\ \mathrm{eV}}), \tag{60}$$

where μ_{Bohr} is the Bohr magneton. Although quite minuscule, several extensions to the SM could dramatically increase this : supersymmeteric models can produce $10^{-14}\mu_{Bohr}$ to $10^{-12}\mu_{Bohr}$ [41] and calculations that invoke large extra dimensions easily yield $10^{-11}\mu_{Bohr}$ or larger [42].

Relative to the SM expectation (60, above), the excluded values of NMM are not at all stringent, being seven to nine orders of magnitude larger. The current limits on neutrino magnetic moment from laboratory experiments are $\mu_\nu \leq 1.5$ to $1.8 \times 10^{-10}\mu_{Bohr}$ for electron neutrinos [43][44] and $\mu_\nu \leq 7.4 \times 10^{-10}\mu_{Bohr}$ for muon neutrinos [45]. Astrophysical limits are stronger: the slow rate of plasmon decay in horizontal branch stars [46] implies $\mu_\nu \leq 10^{-11}\mu_{Bohr}$, while the neutrino energy loss rate from supernova 1987a [47] yields $\mu_\nu \leq 10^{-12}\mu_{Bohr}$. Note, however, that several assumptions are implicit to the astrophysics limits, including the core temperature of the stars; if stellar models omit important processes, these limits may be overestimated. Also, the supernova limit applies only to Dirac neutrinos and not to the Majorana case.

Existing search schemes possess a weakness that sharply limits their ultimate sensitivity: the formulae for the hypothesized effect are quadratic in μ_ν but linear in terms of the experimenter–controlled parameters. In contrast, the following scheme is quadratic in terms of the product of the NMM and a magnetic field strength, $\mu_\nu \cdot$B; hence a carefully designed and executed experiment could improve the limits from current experiments and possibly the limits from astrophysics calculations or actually detect a NMM.

The energy E of a neutrino with a magnetic moment in a magnetic field B gains a new term $\mu_\nu \cdot$B. Consider a B field along the x-axis, and a neutrino with momentum and helicity along the z-axis at $t = 0$. The eigenstates of the neutrino are projections along the x-axis, and the state of the neutrino is expressed as:

$$|\uparrow\rangle = \frac{e^{-i(E+\mu_\nu B)t}}{\sqrt{2}}\,|\leftarrow\rangle + \frac{e^{-i(E-\mu_\nu B)t}}{\sqrt{2}}\,|\rightarrow\rangle\,. \tag{61}$$

As the neutrino propagates, the relative phase of the two components changes, corresponding to a rotation to a sterile state in the case of a Dirac neutrino or to an antineutrino in the Majorana case. At a far detector, the signal would be a deficit in the number of neutrinos detected or increase in the number of antineutrinos detected with the B field in place compared to the sample detected without the B field turned on.

In this phase rotation scheme, the energy splitting occurs as the neutrino passes through a field gradient and experiences a force $F = \nabla(\mu_\nu \cdot \mathrm{B})$. To preserve this energy difference, which drives the phase difference in the absence of the B-field, the field must be turned off instead of allowing the neutrino to experience the reverse gradient as it exits the field region.

There are thus two basic requirements for the magnetic field:

1) The magnetic field must oscillate such that the neutrino experiences only one sign of the gradient. This study assumes that the neutrino bunch length is small compared to the oscillation length. If this assumption is not true, the effects discussed here will be diluted but the basic conclusions will still apply.

2) The magnetic field must be as strong as possible.

We have explored the possibility [48] of using two existing technologies for the B field: resonant cavities and kicker magnets. In both cases the maximum magnetic field is too small to yield improved magnetic moment limits given realistic equipment. We are exploring configurations involving current sheets

The formula for the number of events lost to sterile states may be expressed very simply as:

$$N_{lost} = N * \sin^2(\mu_\nu \mathrm{B} t) \tag{62}$$

where t is the neutrino flight time from entering the magnetic field to detection. We note that, in contrast to an oscillation disappearence signal, this effect is explicitly independant of the neutrino energy. Figure 10 compares the number of events that vanish because of phase rotations to the expected statistical fluctuations in the number of CC events (N) observed in a 50 kton [49] far detector. We see that for a 10 T field gradient and

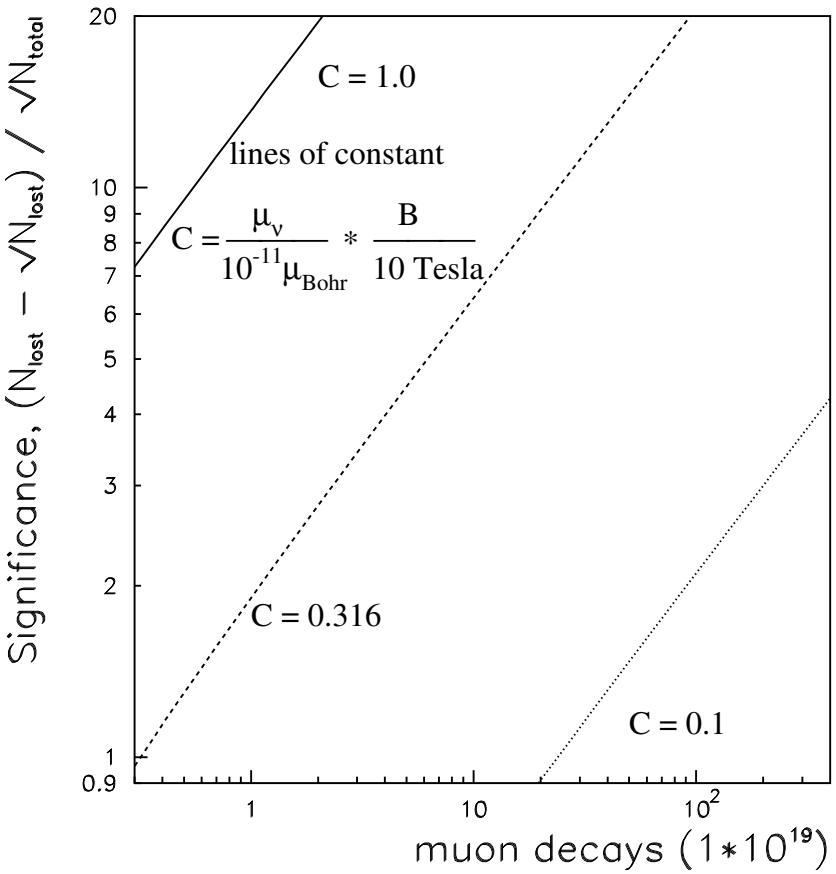

Figure 10: Significance for several scenarios.

10^{19} muon decays we expect a $> 10\sigma$ significance for a NMM of $10^{-11}\mu_{Bohr}$. With a 3T gradient, the limit drops below two sigma. The sensitivity can be increased very strongly by increasing the field strength and more weakly by increasing the number of events in the far detector. Because the detector distance deterimines both t and N in Eqn. 62, the "significance" in the figure is linearly dependent on distance.

To conclude, we have discussed a novel neutrino magnetic moment search technique that uses oscillating magnetic fields at the source of a long baseline detector's neutrino beam. This is the only technique we know of that is quadratic in both μ_ν and a controllable parameter, and thus has the potential for arbitrary sensitivity as we improve our ability to create oscillating magnetic field gradients.

Anomolous Lepton Production

The neutrino beam from a muon storage ring would consist of a virtually pure combination of $\bar{\nu}_e$ and ν_μ (or charge-conjugate). Also, at the source of the neutrino beam, the $\bar{\nu}_e$ and ν_μ will not have had time to oscillate into other flavors: For a 20 GeV muon storage ring with a 700 m straight section, and neutrino oscillations with $\Delta m^2 = 3.5 \times 10^{-3}$ eV^2, the oscillation probability is $\approx 5 \times 10^{-9}$. Furthermore, the neutrino flux is highest at the source. Thus, an experiment at the neutrino source could be highly sensitive to exotic processes resulting in production of e^-, μ^+, or τ of either charge. While such a search is interesting in its own right, it is also useful to rule out exotic contributions to long-baseline neutrino oscillation signals.

These exotic processes would probably have a flat or rising dependence on the neutrino energy E_ν. In contrast, a neutrino oscillation would have a $1/E_\nu^2$ dependence. Also, if the distance L of the experiment changes, the rate of exotic events would decrease with the flux as $1/L^2$. In contrast, the neutrino oscillation probability would increase as L^2 (for L small compared to the oscillation period), and so the rate of oscillated events would be independent of L. Thus, one could distinguish between exotic processes and the beginning of a neutrino oscillation.

Anomalous lepton production could occur if muons decay to neutrino flavors other than those in the usual decay $\mu \to e\bar{\nu}_e\nu_\mu$, and the anomalous neutrinos then interact in the target. Alternatively, they could be produced

if a $\bar{\nu}_e$ or ν_μ interacts with the target via an exotic process.

The only direct experimental limit on exotic $\mu \to e\bar{\nu}_x\nu_y$ decays is $BR(\mu \to e\bar{\nu}_\mu\nu_e) < 1.3\%$[50]. Indirect limits are also very weak. The contribution of non- $V-A$ interactions to the muon decay rate has been limited to 8%[50]. Also, the total muon decay rate is one of the main measurements used to constrain electroweak parameters[50]. To first order,

$$\frac{1}{\tau_\mu} = \frac{G_F m_\mu^5}{192\pi^3}. \tag{63}$$

Assuming the standard model, G_F is determined to 1 part in 10^5 from muon lifetime measurements. If there are exotic contributions to the muon lifetime, the measured value of G_F would be shifted from the true value. Since

$$m_W \propto G_F^{-1/2}, \tag{64}$$

the 0.1% uncertainty on m_W corresponds to a 0.4% shift in the muon lifetime. Finally, the CKM matrix element V_{ud} is determined from the rate of nuclear β-decays relative to the muon lifetime. The assumption of unitarity on the CKM matrix gives us the following constraint on the first row:

$$|V_{ud}|^2 + |V_{us}|^2 + |V_{ud}|^2 = 1. \tag{65}$$

The experimental determination is[50]:

$$|V_{ud}|^2 + |V_{us}|^2 + |V_{ud}|^2 = 0.991 \pm 0.005. \tag{66}$$

The uncertainty on this constraint corresponds to a 0.5% shift in the muon lifetime. Additional contributions to the muon decay rate would lead to a downward shift in the determined value of $|V_{ud}|^2$ from the true value. We conclude that exotic decay modes of the muon with branching ratios totaling 0.5% are possible without contradicting current measurements or tests of the standard model.

As a concrete example of such an exotic process we consider R-parity-violating supersymmetric models. These models lead to lepton-number-violating vertices with couplings λ, and muon decay processes such as $\mu \to e\bar{\nu}_\tau\nu_\tau$ as shown in Fig. 1. The matrix element for these decays turns out to have the same form as for the standard W-exchange. The current constraints on the couplings λ are reviewed in Ref. [51]. These constraints allow a branching ratio of 0.4% for the process in Fig. 11.

Similar processes are allowed for anomalous lepton production as shown for example in Fig. 11. Estimates for allowed rates are in progress [52]. These diagrams involve the λ' couplings. Currently, the best limit on one of these couplings, λ'_{231}, is from ν_μ deep-inelastic scattering, so existing neutrino data is already providing constraints! The search for these types of effects at the muon storage ring could be input into a decision on whether to build a muon-proton collider where they could be studied in more detail.

As a start on estimating the capabilities of an experiment at the neutrino source, we consider the detector concept illustrated in Fig. 12. This concept consists of a repeating sequence of 1.5 mm-thick Tungsten sheets with Silicon tracking, separated by 4 mm. Tungsten, being dense, provides a high target mass while being thin enough for a produced τ to have a high probability of hitting the Silicon. The impact parameter of the τ decay products is typically 90 microns with a broad distribution, so we would like a hit resolution of 5 microns or better. Although there is a lot of multiple scattering in the tungsten, the short extrapolation distance provides for a good impact parameter resolution on the τ decay products. This configuration has been optimized for a 50 GeV muon beam. For lower energy beams, the planes should be spaced more closely, and the Tungsten thickness perhaps reduced. Studies of detectors with passive target mass and tracking with emulsion sheets [53] suggest that we can expect τ reconstruction efficiencies as high as 30%.

We would propose placing such a detector in a magnetic field, and measuring the momentum of muons and hadrons should be straightforward. However, each Tungsten sheet is 0.4 radiations lengths thick, and while we should obtain good energy resolution for electromagnetic showers, determining the electron charge will be difficult. We estimate it would take roughly a 4 Tesla field transverse to the beam direction to have a good chance of measuring the charge of a 50 GeV electron. Even then, detailed studies are needed to determine if this can be done reliably.

A total mass of 6 tons of Tungsten corresponds to 200 m^2 of Silicon tracking. For 5×10^{20} muon decays at 50 GeV, we expect a total of 35 billion neutrino interactions. Obviously there is much potential for sensitivity to very rare exotic processes, but detailed simulations and studies of possible Silicon tracking technologies are needed to quantify this.

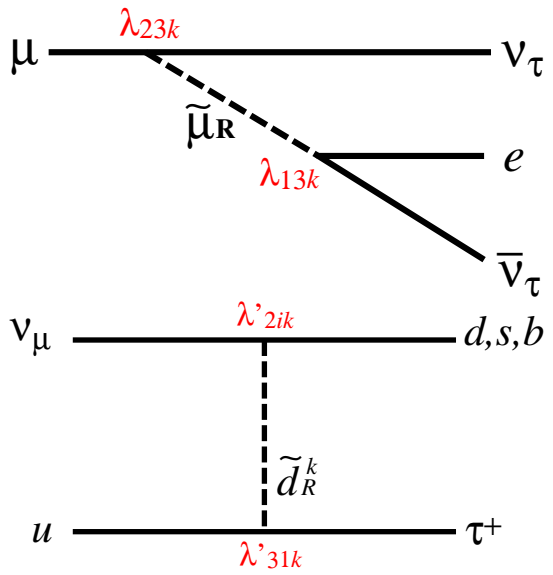

Figure 11: Example of exotic muon decay in R-parity-violating SUSY (Left), and an example of an exotic neutrino interaction in R-parity-violating SUSY (Right).

3 Summary

We have investigated possible conventional neutrino physics studies done at a detector located near a muon storage ring. We emphasized novel methods rather than extensions of existing experiments with additional statistics.

For a reference machine with 50 GeV stored muons and 10^{20} muon decays per year we find that it is possible to:

- Measure individual parton distributions within the proton for all light quarks and anti-quarks.
- Determine the effects of a nuclear environment on individual quark species.
- Measure the spin contributions of individual quark species, including strange quarks and do precision studies of the QCD evolution of spin effects without a need for data from beta decay measurements.

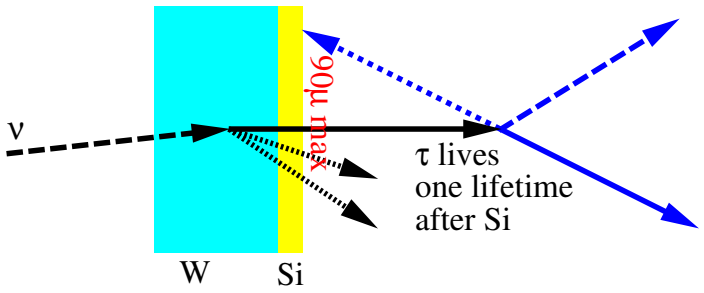

Figure 12: One plane of a detector for τ production.

- Measure charm production with raw event rates of up to 100 million charm events/year with $\simeq$ 2M double tagged events.
- Measure the Weinberg angle in both hadronic and purely leptonic modes with a precision of 0.0001 to 0.0002.
- Search for the production and decay of neutral heavy leptons with mixing angle sensitivity 2 orders of magnitude better than present limits in the 30-80 MeV region.
- Search for a neutrino magnetic moment which may be much large than the Standard Model prediction in some supersymmetric theories.
- Search for anomolous tau production predicted by some R-parity violating supersymmetric models.

We note that the event rates at a near detector increase linearly with neutrino energy. In addition, the acceptance of small detectors is better for the narrower beam produced by higher energy machines. Almost all of the above measurements, with the exception of the neutral heavy lepton search, lose sensitivity if the beam energy is less than 50 GeV and gain if it is greater.

References

References

[1] S. Adler, Phys.Rev.143, (1966), 1144-1155.

[2] C. Boros et al., hep-ph/9810220, Oct. 1998.

[3] S.A. Kulagin, hep-ph/9812532, Aug. 1998.

[4] K.J. Eskola et al. hep-ph/9906484, May, 1999.

[5] K. McFarland *et al.*, Eur. Phys. J. **C1** (1998) 509.

[6] P. Vilain *et al*, Phys. Lett. **B335** (1994) 248.

[7] "The Potential for Neutrino Physics at Muon Colliders and Other Muon Storage Rings", B. King *et al*, to appear in *Physics Reports*.

[8] ICANOE Proposal, CERN/SPSC 99-25.

[9] Bruce King, "High Rate Physics at Neutrino Factories", Proc. 23rd Johns Hopkins Workshop on Current Problems in Particle Theory, `hep-ex/9911008`.

[10] E. Aitala *et al*, Phys. Rev. **D57** (1998) 13.

[11] M. Artuso *et al*, "Search for $D^0 - \overline{D^0}$ Mixing", `hep-ex/9908040`.

[12] P. F. Harrison and H. R. Quinn [BABAR Collaboration], "The BaBar physics book: Physics at an asymmetric B factory," SLAC-R-0504.

[13] Bruce King, "High Rate Neutrino Detectors for Neutrino Factories", Proc. ICFA/ECFA Workshop "Neutrino Factories based on Muon Storage Rings" (nuFACT'99), `hep-ex/0001043`.

[14] K. McFarland *et al.*, Eur. Phys. J. **C1** (1998) 509.

[15] "The Potential for Neutrino Physics at Muon Colliders and Other Muon Storage Rings", B. King *et al*, to appear in *Physics Reports*.

[16] P. Vilain *et al*, Phys. Lett. **B335** (1994) 248.

[17] ICANOE Proposal, CERN/SPSC 99-25.

[18] C.Arroyo, B.J.King *et. al.*, Phys. Rev. Lett. **72**, 3452 (1994).

[19] K.S.McFarland *et al.*, CCFR, Eur. Phys. Jour. **C1**, 509 (1998)

[20] C.H.Llewellyn Smith, Nucl. Phys. **B228**, 205 (1983)

[21] R.Bernstein *et. al.*, NuTeV Collaboration, Fermilab-TM-1088 (1994).

[22] E.A.Paschos and L. Wolfenstein, Phys. Rev. **D7**, 91 (1973)

[23] K.S.McFarland, NuTeV collaboration, to be published in the proceedings of the XXXIIIrd Rencontres de Moriond (1998); J. Yu, NuTeV collaboration, to be published in the proceedings of the DIS98, Brussel, Belgium, Fermilab-Conf-98/200-E (1998)

[24] H. Schellman, to be published in the proceedings of the Workshop on Physics at the First Muon Collider, Fermilab, Batavia, IL, USA, Nov. 1997.

[25] D.A.Harris & K.S.McFarland, MIT-LNS-98-276, to be published in the proceedings of the Workshop on Physics at the First Muon Collider, Fermilab, Batavia, IL, USA, Nov. 1997

[26] B.J.King, to be published in the proceedings of the Workshop on Physics at the First Muon Collider, Fermilab, Batavia, IL, USA, Nov. 1997.

[27] U.K Yang and A. Bodek, *UR-1543*, Submitted to Phys. Rev. Lett, hep-ex/9809480 (1998)

[28] U. Baur and M. Demarteau, "Precision Electroweak Physics at Future Collider Experiments," Fermilab-Conf-96/423 (1996).

[29] P. Villain *et al.*, Phys. Lett. **B335**:246 (1994). See also Phys. Lett. **B302**:351 (1993) and Phys. Lett. **B281**:159 (1992).

[30] D. Yu. Bardin and V. A. Dokuchaeva, JINR E2-86-260 (1986).

[31] U. Baur, "Electroweak Radiative Corrections to W Boson Production at the Tevatron", SUNY-Buffalo preprint UB-HET-98-02, Sep 1998 (e-Print Archive: hep-ph/9809327).

[32] E. Sather, Phys. Lett. **B274** (1992) 433.

[33] M.Gronau, C.N. Leung, and J.L. Rosner, Phys. Rev. **D29**, 2539 (1984).

[34] R. E. Shrock, Phys. Rev. **D24**, 1232 (1981).

[35] T. Bolton, L. Johnson, and D. McKay, Phys. Rev. D **56** (1997) 2970.

[36] A. Vaitaitis *et al.*, Phys. Rev. Lett. **83** (1999) 4943.

[37] J. Formaggio *et al.*, Phys. Rev. Lett. **XXX** (2000) XXX.

[38] *Review of Particle Physics* Eur. Phys. J. C. 3,320 (1998).

[39] R. Shrock, Phys. Rev. D **24** (1981) 1232.

[40] B.W.Lee and R.E.Shrock, Phys. Rev. **D16** 1444 (1977).

[41] M.Frank, Phys. Rev. D60:093005 (1999).

[42] G.C.McLaughlin and J.N.Ng, hep-ph/9909558.

[43] J.F.Beacom and P.Vogel, Phys. Rev. Lett. **83**, 5222 (1999).

[44] A.V.Derbin, Phys. of Atomic Nuclei, **57**, 222 (1994) [Yad. Fiz. **57**, 236 (1994)], and A.I.Derbin *et al.,* JETP Lett. **57**, 768 (1993).

[45] D.A.Krakauer *et al.*, Phys. Lett. **B252**, 177 (1990); R.C.Allen *et al.*, Phys. Rev. **D47**, 11 (1993).

[46] MFukugita and S.Yazaki, Phys. Rev. **D36** (1987) 3817.

[47] R.Barbieri and R.N.Mohapatra, Phys. Rev. Lett. **61** (1988) 27, and J.M. Lattimer and J.Cooperstein, Phys. Rev. Lett. **61** (1988) 23.

[48] Private discussions with Norbert Holtkamp, Fermilab.

[49] See Steve Geer's talk at the 2-day meeting. Number of events (5000) was quoted for a 50 kTon detector at L=2800 km and a 20 GeV muon storage ring.

[50] Review of Particle Properties, C. Caso *et. al.*, Euro. Phys. J. **C**3, 1 (1998).

[51] H. Dreiner, hep-ph/9707435

[52] Chris Quigg, private communication

[53] K. Kodama *et. al.* (OPERA Collaboration), CERN/SPSC 98-25.
A. E. Asratyan *et. al.*, hep-ex/0002019

Table 1: Charged current muon-neutrino scattering rates in a small target located near a muon storage ring. Rates are per 10^{20} muon decays. The detector is located (E_μ, GeV) meters away from the ring to assure that primary muons have ranged out before the detector.

Machine	Target	Thickness,cm	Events
50 GeV neutrino factory	Liquid H_2	100	12.1M
	Liquid D_2	100	29.0M
	solid HD	50	9.3M
	C	5.3	20.7M
	Si	6.3	25.4M
	Fe	2.3	31.6M
	Sn	3.1	39.1M
	W	1.3	44.3M
	Pb	2.4	46.5M
CCFR/NuTeV	Fe	600	$\sim$ 2M

Table 2: g_L and g_R by $\nu - e$ scattering process

Reaction	g_L	g_R	$g_L^2 + \frac{1}{3}g_R^2$
$\nu_\mu e^- \to \nu_\mu e^-$	$-\frac{1}{2} + \sin^2\theta_W$	$\sin^2\theta_W$	0.0925
$\nu_e e^- \to \nu_e e^-$	$\frac{1}{2} + \sin^2\theta_W$	$\sin^2\theta_W$	0.5425
$\bar{\nu}_\mu e^- \to \bar{\nu}_\mu e^-$	$\sin^2\theta_W$	$-\frac{1}{2} + \sin^2\theta_W$	0.0758
$\bar{\nu}_e e^- \to \bar{\nu}_e e^-$	$\sin^2\theta_W$	$\frac{1}{2} + \sin^2\theta_W$	0.2258